Reliable inkjet printing of chondrocytes and MSCs using reservoir agitation

Reliable inkjet printing of chondrocytes and MSCs using reservoir agitation

Joseph P. R. Dudman[1], Ana Marina Ferreira[1], Piergiorgio Gentile[1], Xiao Wang[2] Ricardo da Conceicao Ribeiro[1], Matthew Benning[1] and Kenneth W. Dalgarno[1]

[1] School of Engineering, Newcastle University, United Kingdom
[2] Institute of Cellular Medicine, Newcastle University, United Kingdom

Abbreviations

DoD – Drop-on-Demand
MSC – Mesenchymal Stromal Cell

Keywords

Bioprinting; Drop-on-demand; Mesenchymal Stromal Cell; Chondrocyte; Inkjet; Liquid handling

Abstract

Drop-on-demand (DoD) inkjet printing has been explored for a range of applications, including those to selectively deposit cellular material, due to the high accuracy and scalability of such systems when compared with alternative bioprinting techniques. Despite this, there remains considerable limitations when handling cell suspensions due to the agglomeration and sedimentation of cells during printing, leading to a deterioration in jetting performance. The objective of this work was to design and assess the effectiveness of a custom agitation system to maintain cellular dispersion within the ink reservoir during printing. The cell printing performance of an inkjet printer was assessed with and without the use of a custom agitation system, with biological characterisation performed to characterise the impact of the agitator on cellular viability and function. Cell printing performance was retained over a 2-hour printing period when incorporating an agitated reservoir, with a gradual reduction in performance observed under a non-agitated configuration. Cell assays indicated that the agitation process did not significantly affect the viability, metabolic activity or morphology of the mesenchymal stromal cell or chondrocyte cell types. This study therefore provides a new methodology to increase process reliability within DoD printing platforms when jetting cellularised material.

Introduction

Drop-on-demand (DoD) bioprinting technologies show significant potential for tissue engineering applications due to the inherent scalability and resolution associated with such processes. Most

commonly, DoD methodologies incorporate both valve and inkjet actuated dispensing systems to sequentially deliver low volumes of biological material onto a substrate in a spatially defined pattern. Of these techniques, inkjet printing provides the highest potential resolution due to the ability to deposit individual droplets at volumes within the picolitre-scale (Liu & Derby, 2019).

Inkjet printing processes operate through the application of an actuation signal, a drive waveform, to the piezoelectric element within the jetting device. This results in changes to the materials shape as a function of the waveform intensity and polarity, resulting in the expansion or contraction of the nozzle capillary. Volume changes within the capillary result in the formation of pressure propagations within the fluid that leads to droplet ejection and subsequent refilling of the nozzle. The drive waveform applied to the device represents the intensity, duration and polarity of the electrical signal applied to the actuator and is used to modulate droplet ejection behaviour (Kwon, 2010). This is shown in Figure 1.

A variety of previous research has explored the performance of inkjet printing processes for the deposition of cellular material. This includes the ability to spatially dispense cellular material at the single cell scale, as well as generate complex 2-dimensional patterns through dispensing a combination of different cell types onto a single substrate with a high degree of accuracy (Yusof et al., 2011; Park et al., 2017; Xu et al., 2005; Lorber et al., 2014; Yamaguchi et al., 2012; Tse et al., 2016; Roth et al., 2004; Liberski et al., 2011). Both academic and commercial research have embraced the fields of high-throughput screening and microfluidic liquid handling systems due to the high costs and low success rate associated with drug discovery (Paul et al., 2010; DiMasi et al., 2016). As a result, over the previous decades there has been growing interest in techniques that are able to dispense low volumes of biological material for drug screening applications, thus enabling a reduction in experimental size and cost whilst simultaneously increasing the scale at which screening experiments can be conducted (Burbaum, 1997, 1998; Mayr & Fuerst, 2008; Szymański et al., 2012; Hassig et al., 2014). Of these processes, inkjet printing has been demonstrated to provide a viable method to deposit small quantities of material for high-throughput drug screening applications (Lemmo et al., 1998; Niles & Coassin, 2005; Kong et al., 2012).

Despite this, a number of studies have highlighted challenges associated with the use of inkjet printing devices for dispensing cellular material. This includes inherent limitations to the technology such as the maximum ink cell concentration that can be deposited when using nozzles with small orifice diameters (Cui et al., 2010). In addition, drawbacks surrounding the sedimentation of cellular material within the nozzle prior to and during printing has been demonstrated to reduce device jetting performance (Chahal et al., 2012). Cellular agglomeration through cell-to-cell contact has also been reported, increasing the dimensions of cellular material and thus reducing the propensity of cell ejection from the nozzle orifice (Parsa et al., 2010). As a consequence, inkjet printing techniques are currently limited to exploratory research applications whereby the reliability issues surrounding the technique can be circumvented through using short printing windows and low ink cell concentrations. These factors result in limitations being placed on the maximum density and size of printed tissues when using inkjet printing techniques (Cui et al., 2010; Chahal et al., 2012).

Previous research has explored the use of buoyancy suspensions and agitation within the ink solution immediately prior to printing in an attempt to circumvent such issues. However, such methodologies have been reported to have mixed effects on printing performance, with modifications to the ink suspension and agitation conditions having potential implications on cellular viability or ink rheology and subsequent jetting behaviour (Chahal et al., 2012; Parsa et al., 2010). Further research is therefore required to design and benchmark a system to control cell sedimentation without implicating biological function or ink printability.

Here, we present a methodology to improve the performance of the inkjet printing process through utilising a custom reservoir agitation system to reduce cellular sedimentation and agglomeration effects. An agitated reservoir and purging protocol is benchmarked with a regular printing setup to quantify its effect on cell printing performance. Mesenchymal stromal cell (MSC) and chondrocyte cell lines are printed to determine the suitability of the printing process for cartilage tissue engineering applications. Cellular viability, metabolic activity and morphology were assessed following printing, indicating that the agitation process has no significant effects across the assessment period for either cell type. Following an assessment of the biological impact, single cell printing performance is characterised under an agitated reservoir configuration to enable the spatial deposition of single cells.

Methodology

Cell Culture

Y201 hTERT immortalised human MSCs were cultured in high glucose (4.5 g / L) Dulbecco's Modified Eagle Medium (DMEM; Thermo Fisher Scientific, USA) supplemented with 10 % foetal bovine serum (Thermo Fisher Scientific), 5000 U / mL Penicillin / Streptomycin (Sigma-Aldrich, UK) and 2 mM L-Glutamine (Sigma-Aldrich). TC28a2 human chondrocyte cells (Merck, USA) were cultured in high glucose (4.5 g / L) DMEM / Ham's F12 mix 1:1 v / v (Thermo Fisher Scientific) supplemented with 10 % foetal bovine serum (Thermo Fisher Scientific), 5000 U / mL Penicillin / Streptomycin (Sigma-Aldrich) and 2 mM L-Glutamine (Sigma-Aldrich). Both cell lines were incubated at 37 °C, 5 % CO_2 prior to cell printing experiments.

Printing Configuration

Printing was performed using a JetLab® 4 XL (MicroFab, USA) printing work station combined with a JetDrive® printer drive electronics unit. The system was controlled using coordinate-based jetting commands and a single deposition location was programmed for each sample print run. Under this configuration, the actuation cycle number at each coordinate was used to control the total volume of material dispensed into each well. The printing performance of unipolar and bipolar waveform designs were compared in response to variations in the waveform dwell time, defined as the period in which a constant voltage is applied to the inkjet actuator in order to achieve droplet ejection. The unipolar waveform design consisted of a positive pulse followed by a neutral period, with the bipolar design also featuring a negative pulse between the positive pulse and neutral period. Printing was performed at an actuation frequency of 1000 Hz.

An MJ-AT-01 threaded single-orifice piezoelectric jetting device (MicroFab, USA) featuring a 60 µm orifice diameter was used to deposit material from the printer reservoir. The on-board pneumatic regulator was controlled via the JetDrive® control software to provide a negative backpressure within the reservoir of between -0.1 and -0.3 psi. The pressure level was adjusted prior to each print job to ensure that the ink meniscus at the nozzle tip remained flush with the orifice.

The system was cleaned by flushing 1 % v / v Micro-90 cleaning solution (Cole-Parmer, USA) followed by 70 % v / v ethanol (Fisher Scientific) through the reservoir, tubing and jetting device immediately prior to and following printing to remove any potential sources of contamination.

Cell specific cell culture medium was used as the bioink in each of the bioprinting experiments. The solution was heated to 37 °C and filtered using a 0.22 µm filter (Merck) prior to use. Cell pellets were re-suspended within the culture media formulation and transferred to the reservoir for printing.

Agitator Design and Fabrication

The performance of two individual agitated reservoir designs were assessed within this study. Both designs featured a MINSTAC® 062 thread (the Lee Company, USA) to enable direct coupling with the inkjet actuator. Ink was supplied from both reservoir designs via the lowest point within the reservoir volume. A continuous voltage of 1.5 V was applied to the motor of either device via an external power supply unit (Elenco Electronics, USA) following ink loading to control cell sedimentation. Both agitators were designed in-house and manufactured externally using a 3D printing production company (Protolabs, USA).

Agitator design 'A' featured a shaft-driven axial-flow impeller attached to an electric motor mounted directly above the 2 mL capacity ink reservoir, as shown in Figure 2. Cell loading was performed by decoupling the agitator and reservoir components, with pressure controlled via an externally mounted push-fit pneumatic tube connector.

Agitator design 'B' was comprised of a 5 mL capacity reservoir containing an internally mounted gold-plated cylindrical neodymium magnet, as shown in Figure 3. Rotation was induced via an externally mounted electrical motor coupled to an additional magnet. Within this design the ink and actuator were independently sealed to minimise contamination risk during operation. Ink loading was performed via the removal of a pressure-mounted lid.

Characterisation of Printing Performance

Single cell printing performance was characterised by manually counting the number of cells contained within single droplets sequentially deposited onto a glass slide. Droplet cell concentration was determined immediately following printing using a DMLB microscope (Leica Biosystems, Germany).

Reservoir Cell Sedimentation

The degree of cellular sedimentation within the ink for each reservoir design was quantified by sampling the cell concentration of each reservoir every 15 minutes over a 2-hour duration. Cell number was determined using a 0.1 mm depth Neubauer chamber haemocytometer (Hawksley, UK) in combination with a trypan blue exclusion test. To perform a cell count, a 20 µL aliquot of cell-containing solution was combined with an equal volume of 0.4 % trypan blue staining solution (Sigma-Aldrich), and the viable cell number determined by counting the number of unstained cells.

Cell Viability Assay

A Live / Dead ® cell viability assay was performed to assess the impact of the printing process on cellular viability. Cells were printed or manually pipetted onto glass coverslips for both immediate assessment and analysis after a 24 hour incubation period. Stock solutions were warmed to room temperature and diluted in PBS (Sigma-Aldrich) to produce a 2 µM calcein acetoxymethyl and 4 µM ethidium homodimer-1 working solution. Adherent cells were washed extensively with PBS prior to the application of Live / Dead® working solution (Thermo Fisher Scientific). The samples were incubated for a period of 30 minutes in a humidified atmosphere at 37 °C, 5 % CO_2 prior to imaging. Imaging was performed using a DMLB fluorescence microscope (Leica Biosystems, Germany) at 10x magnification, and images captured using a SPOT Advanced CMOS camera (Spot Imaging Solutions, USA) and corresponding microscopy software.

Metabolic Activity Assays

An MTT assay was performed to compare the metabolic activity of printed and manually pipetted cells when seeded into the wells of a 96 well plate.. Following incubation for each time point, the cell supernatant from each well was removed and replaced with 100 µL of freshly prepared MTT (Sigma-

Aldrich) working solution (0.5 mg / mL) in phenol-red free cell culture media (Thermo Fisher Scientific). Plates were incubated for 4 hours until formazan crystals had been produced. The supernatant was then removed from each well and replaced with 100 µL of propan-2-ol detergent solution (Fisher Scientific, USA). The plate was agitated for 30 minutes to solubilise the formazan crystals. The absorbance values for each well were obtained using an ELx800 microplate reader (Biotek, USA) at 570 nm with a 630 nm reference wavelength recorded for normalisation.

A PrestoBlue® assay was performed to monitor the metabolic activity of agitated and non-agitated samples over a 2-hour incubation period. Cell samples were dispensed into the wells of a 96 well plate containing 100 µL of PrestoBlue® (Thermo Fisher Scientific) working solution previously prepared from the addition of 10 % v / v PrestoBlue® reagent to phenol-red free cell culture media. Plates were incubated for 4 hours and fluorescence values then obtained using a FLUOstar® Omega microplate reader (BMG Labtech, Germany) using an excitation and emission filter of 544 nm and 620 nm respectively.

Visualisation of Cell Morphology

Cell morphology was visualised using a combination of phalloidin–tetramethylrhodamine B isothiocyanate (Sigma-Aldrich) and 4',6-diamidino-2-phenylindole (DAPI; Sigma-Aldrich) fluorescence stains to indicate cytoskeletal filamentous actin and cell nuclei respectively. Cells were printed or manually pipetted onto glass coverslips, which were incubated for the respective period of time prior to being fixed in 4% paraformaldehyde solution (Thermo Fisher Scientific) for staining. Fixed cells were washed extensively in PBS prior to the addition of 1 µg / mL phalloidin working solution prepared in PBS. Cells were incubated for a period of 20 minutes at room temperature prior to three washes in PBS. Coverslips were then mounted onto glass slides via the addition of mounting media containing DAPI and visualised using an LSM800 point scanning confocal microscope (Carl Zeiss AG) at 20x magnification.

Statistical Analysis

Data presented shows mean values ± standard deviation. All data were analysed using Prism® 8 statistical analysis software (GraphPad Software, USA) using two-way analysis of variance in combination with Tukey or Šídák multiple comparison tests. Levels of statistical significance were defined using $P \leq 0.05$ (*), $P \leq 0.01$ (**) and $P \leq 0.001$ (***).

Results and Discussion

Waveform Development

The jetting performance of unipolar and bipolar waveform designs were benchmarked in response to different dwell time configurations when depositing cell culture media. Bipolar waveform designs were shown to consistently operate across a greater dwell time range than unipolar designs (Figure 4), thus providing increased versatility for cell printing applications. A maximum droplet ejection velocity of 6 ms^{-1} was achieved at a dwell time of approximately 30 µs when using the bipolar design. All subsequent experiments were performed using the bipolar waveform with a 30 µs dwell time to maintain the 6 ms^{-1} droplet ejection velocity.

Agitator Benchmarking

Figure 5 compares the performance of agitator designs A and B, manually agitated samples via repeated aspiration and deposition using a pipette, and non-agitated samples. For both the MSC and chondrocyte cell lines, the incorporation of an automated agitation technique was shown to substantially reduce the rate of cellular sedimentation over the 2-hour incubation period assessed. A significant reduction in cell number per sample was observed for the non-agitated sample over the

course of 45 minutes, resulting in no cellular material being collected throughout the remainder of the time course. Both agitator designs demonstrated a similar number of cells per sample throughout the incubation period, with no discernible reduction in cell density observed when compared to manually agitated samples. These results demonstrate the suitability of each design for the maintenance of homogenous cellular dispersion within a bioink solution.

Analysis of the impact of the agitation system on cellular metabolic activity for each sample revealed a significant reduction in the metabolic activity of samples collected from the non-agitated reservoir, which can be attributed to the reduction in cell density collected at each time point. Statistically significant variations in metabolic activity were observed across a greater number of time points when using agitator design A versus B for both cell lines, with the metabolic activity of samples agitated using design B most closely aligning with the manually agitated control samples. In combination, these observations indicate that agitator design B is most suitable for cell printing applications due to the reduced impact of the design on cellular metabolic activity.

It was also important to consider the impact of the ink working volume and agitation device usability for bioprinting applications. Due to the larger design volume, agitator B was capable of dispensing greater volumes of material prior to refilling. In addition, the upper inlet port enabled the refilling of the reservoir design without requiring disassembly. When combined with the externally sealed motor design, these modifications reduced the potential for contamination, as well as reducing both the labour time and potential for component damage when refilling the reservoir. Minimum ink working volumes are also of particular importance for biofabrication applications where high value reagents or low volume print jobs are required. Agitator design B featured a larger cylindrical agitator which required continual immersion within the ink to avoid bubble formation. For agitator A the impellor also had to be kept fully immersed to avoid bubble formation, but this could be achieved with a smaller volume of fluid. As a result, the minimum working ink volume required for operation was significantly larger than for the impellor design of agitator A.

Purging the nozzle immediately prior to printing was also shown to reduce the variability in cell concentration dispensed during subsequent printing. It is hypothesised that this was due to the dead volume of non-agitated material between the reservoir chamber and the nozzle tip being removed prior to printing. When no printing is taking place, sedimentation can occur leading to variations in ink cell density. These results highlight the importance of considering the sedimentation tendency of cellular material throughout the printing process and provide a potential mechanism to minimise such effects. It was not possible to further reduce this volume based upon the connection requirements and design of the actuator, and therefore purge cycles were implemented immediately prior to printing in order to minimise these effects within future experiments.

Agitator design B was benchmarked against a non-agitated reservoir design to evaluate its impact on cell printing performance. Consistent cell printing performance was demonstrated within agitated samples throughout the 2-hour printing duration, with non-agitated samples displaying a marked reduction in density until printing failure at approximately 75 minutes. This was caused by a cell-induced nozzle blockage as depicted in Figure 6. These findings reinforce previous observations that have reported variations in printing performance when using non-agitated versus modified printing setups (Saunders et al., 2008; Parsa et al., 2010; Chahal et al., 2012; Tse et al., 2016).

These results demonstrate that the agitation technique can be used alongside appropriately defined purge cycles to maintain cellular dispersion during printing, without altering ink composition or requiring significant printer modification.

Biological Impact Assessment

The biological impact of the agitated printing process was assessed via a combination of cellular viability, morphology and metabolic activity assays, as displayed in Figure 7 for MSC and chondrocyte cell types. Cell viability assay data displayed no discernible difference in the proportion of live to dead cells within printed and manually deposited samples, both immediately following and 24 hours after printing, irrespective of the cell line assessed. In addition, the printing process was shown to have no significant impact on the metabolic activity of either cell line when compared with manual dispensing techniques. Comparisons between the morphology of printed and manually deposited MSC and chondrocyte cells revealed no discernible difference in cell size, morphology or substrate adherence. In combination, these data demonstrate the suitability of the printing platform for the selective deposition of MSC and chondrocyte cell types, providing potential applications within the field of cartilage tissue engineering. These results corroborate with previous research demonstrating the compatibility of the inkjet printing process with other cell types (Saunders et al., 2008; Tse et al., 2016). In addition, they provide the first example of inkjet printed Y201 MSC and TC28a2 chondrocyte cell lines.

Single Cell Printing Performance

Further evaluation of the printing process was performed to determine the maximum possible print resolution that could be attained for each cell type under the previously defined printing parameters and agitation system developed. Figure 8 displays a frequency distribution of the number of cells contained within each dispensed droplet at ink cell concentrations of 1 and 2 million cells per mL. Single cell printing was achieved across the highest proportion of deposited droplets for both the MSC and chondrocyte cell lines at a concentration of 2 million cells per mL, with the ratio of cells per droplet correlating with a Poisson probability distribution. These findings reflect the outcomes of previous research whereby a similar distribution in cells per droplet were identified when using inkjet printing devices to perform single cell printing (Liberski et al., 2011; Yusof et al., 2011; Moon et al., 2011). Furthermore, cell type was not shown to significantly impact the mean cell density per printed droplet, highlighting the versatility of the printing process with different cell types, although we would observe that the cells are of a similar size and that this may result in similar processability. Finally, droplet ejection characteristics were retained to enable the ejection of single droplets with minimal ligand formation per actuation cycle. This prevented a deterioration in printing resolution or accuracy that can occur when depositing droplets with substantial ligands due to the formation of satellite droplets (Kwon, 2010; Liu & Derby, 2019; Jang et al., 2009).

Conclusions

The potential of inkjet bioprinting is well established, but the key to achieving this potential is consistent and reliable performance, which can only be achieved through avoiding agglomeration within the ink. In this research, two custom agitation designs were evaluated in order to reduce the rate of cellular sedimentation within the reservoir of an inkjet bioprinting platform. When combined with a purge cycle to systematically remove any non-agitated material prior to beginning a print, the incorporation of each agitation system was shown to improve printing performance in comparison with a non-agitated design, through minimising the rate of nozzle blockages over a 2-hour printing period. These results provide a novel method to improve inkjet printing performance without altering ink composition, whilst also highlighting the critical design considerations that must be met when developing cell printing equipment. Single cell printing performance was achieved using the agitated inkjet printing platform, providing new opportunities for high resolution (1-2 cells per drop) cell printing over extended time periods. Characterisation of cell viability, metabolic activity and

morphology provides the first reported evidence of the compatibility of the agitated inkjet printing platform with Y201 MSC and TC28a2 chondrocyte cell types.

Acknowledgements

Funding to support this research from (i) the UK EPSRC Centre for Doctoral Training in Additive Manufacture and 3D Printing (EP/L01534X/1) and (ii) the Tissue Engineering and Regenerative Therapies Centre Versus Arthritis (Arthritis Research UK Award 21156), is gratefully acknowledged. Data supporting this publication is openly available under an 'Open Data Commons Open Database License'. Additional metadata are available at https://doi.org/10.25405/data.ncl.11770638.v1.

References

Burbaum, J. (1997) New technologies for high-throughput screening. *Current Opinion in Chemical Biology*. 1 (1), 72–78.

Burbaum, J.J. (1998) Miniaturization technologies in HTS: How fast, how small, how soon? *Drug Discovery Today*. 3 (7), 313–322.

Chahal, D., Ahmadi, A. & Cheung, K.C. (2012) Improving piezoelectric cell printing accuracy and reliability through neutral buoyancy of suspensions. *Biotechnology and Bioengineering*. 109 (11), 2932–2940.

Cui, X., Dean, D., Ruggeri, Z.M. & Boland, T. (2010) Cell damage evaluation of thermal inkjet printed chinese hamster ovary cells. *Biotechnology and Bioengineering*. 106 (6), 963–969.

DiMasi, J.A., Grabowski, H.G. & Hansen, R.W. (2016) Innovation in the pharmaceutical industry: New estimates of R&D costs. *Journal of Health Economics*. 4720–33.

Hassig, C.A., Zeng, F.Y., Kung, P., Kiankarimi, M., Kim, S., Diaz, P.W., Zhai, D., Welsh, K., Morshedian, S., Su, Y., O'Keefe, B., Newman, D.J., Rusman, Y., Kaur, H., Salomon, C.E., Brown, S.G., Baire, B., Michel, A.R., Hoye, T.R., et al. (2014) Ultra-high-throughput screening of natural product extracts to identify proapoptotic inhibitors of Bcl-2 family proteins. *Journal of Biomolecular Screening*. 19 (8), 1201–1211.

Jang, D., Kim, D. & Moon, J. (2009) Influence of fluid physical properties on ink-jet printability. *Langmuir*. 25 (5), 2629–2635.

Kong, F., Yuan, L., Zheng, Y.F. & Chen, W. (2012) Automatic liquid handling for life science: A critical review of the current state of the art. *Journal of Laboratory Automation*. 17 (3), 169–185.

Kwon, K.-S. (2010) Experimental analysis of waveform effects on satellite and ligament behavior via in situ measurement of the drop-on-demand drop formation curve and the instantaneous jetting speed curve. *Journal of Micromechanics and Microengineering*. 20 (11), 115005.

Lemmo, A. V, Rose, D.J. & Tisone, T.C. (1998) Inkjet dispensing technology: Applications in drug discovery. *Current Opinion in Biotechnology*. 9 (6), 615–617.

Liberski, A.R., Delaney, J.T. & Schubert, U.S. (2011) 'One cell-one well': A new approach to inkjet printing single cell microarrays. *ACS Combinatorial Science*. 13 (2), 190–195.

Liu, Y. & Derby, B. (2019) Experimental study of the parameters for stable drop-on-demand inkjet performance. *Physics of Fluids*. 31 (3), 32004.

Lorber, B., Hsiao, W.-K., Hutchings, I. & Martin, K. (2014) Adult rat retinal ganglion cells and glia can be printed by piezoelectric inkjet printing. *Biofabrication*. 6 (1), 15001.

Mayr, L.M. & Fuerst, P. (2008) The future of high-throughput screening. *Journal of Biomolecular*

Screening. 13 (6), 443–448.

Moon, S., Kim, Y.G., Dong, L., Lombardi, M., Haeggstrom, E., Jensen, R. V., Hsiao, L.L. & Demirci, U. (2011) Drop-on-demand single cell isolation and total RNA analysis. *PLoS ONE*. 6 (3), .

Niles, W.D. & Coassin, P.J. (2005) Piezo- and Solenoid Valve-Based Liquid Dispensing for Miniaturized Assays. *Assay and Drug Development Technologies*. 3 (2), 189–202.

Park, J.A., Yoon, S., Kwon, J., Now, H., Kim, Y.K., Kim, W.J., Yoo, J.Y. & Jung, S. (2017) Freeform micropatterning of living cells into cell culture medium using direct inkjet printing. *Scientific Reports*. 7 (1), 14610.

Parsa, S., Gupta, M., Loizeau, F. & Cheung, K.C. (2010) Effects of surfactant and gentle agitation on inkjet dispensing of living cells. *Biofabrication*. 2 (2), 25003.

Paul, S.M., Mytelka, D.S., Dunwiddie, C.T., Persinger, C.C., Munos, B.H., Lindborg, S.R. & Schacht, A.L. (2010) How to improve RD productivity: The pharmaceutical industry's grand challenge. *Nature Reviews Drug Discovery*. 9 (3), 203–214.

Roth, E.A., Xu, T., Das, M., Gregory, C., Hickman, J.J. & Boland, T. (2004) Inkjet printing for high-throughput cell patterning. *Biomaterials*. 25 (17), 3707–3715.

Saunders, R.E., Gough, J.E. & Derby, B. (2008) Delivery of human fibroblast cells by piezoelectric drop-on-demand inkjet printing. *Biomaterials*. 29 (2), 193–203.

Szymański, P., Markowicz, M. & Mikiciuk-Olasik, E. (2012) Adaptation of high-throughput screening in drug discovery-toxicological screening tests. *International journal of molecular sciences*. 13 (1), 427–52.

Tse, C., Whiteley, R., Yu, T., Stringer, J., MacNeil, S., Haycock, J.W. & Smith, P.J. (2016) Inkjet printing Schwann cells and neuronal analogue NG108-15 cells. *Biofabrication*. 8 (1), 15017.

Wu, C.H. & Hwang, W.S. (2015) The effect of the echo-time of a bipolar pulse waveform on molten metallic droplet formation by squeeze mode piezoelectric inkjet printing. *Microelectronics Reliability*. 55 (3–4), 630–636.

Xu, T., Jin, J., Gregory, C., Hickman, J.J.J.J. & Boland, T. (2005) Inkjet printing of viable mammalian cells. *Biomaterials*. 26 (1), 93–9.

Yamaguchi, S., Ueno, A., Akiyama, Y. & Morishima, K. (2012) Cell patterning through inkjet printing of one cell per droplet. *Biofabrication*. 4 (4), 45005.

Yusof, A., Keegan, H., Spillane, C.D., Sheils, O.M., Martin, C.M., O'Leary, J.J., Zengerle, R. & Koltay, P. (2011) Inkjet-like printing of single-cells. *Lab on a Chip*. 11 (14), 2447–2454.

Figures List

Unipolar and Bipolar Waveform Design

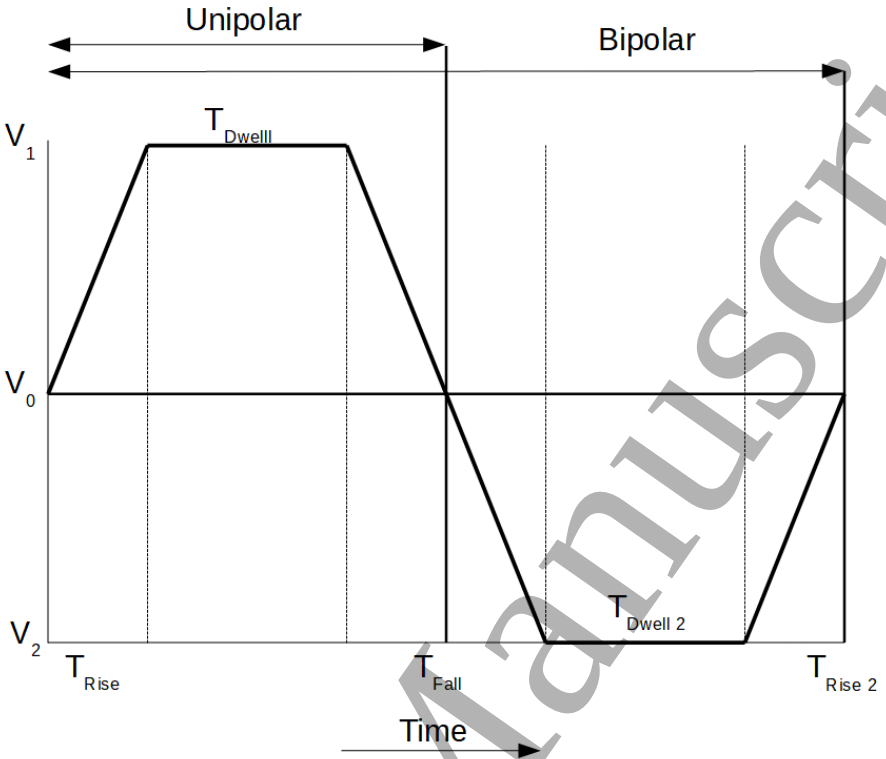

Figure 1 – Unipolar and bipolar piezoelectric waveform designs.

Agitator Design A Diagram

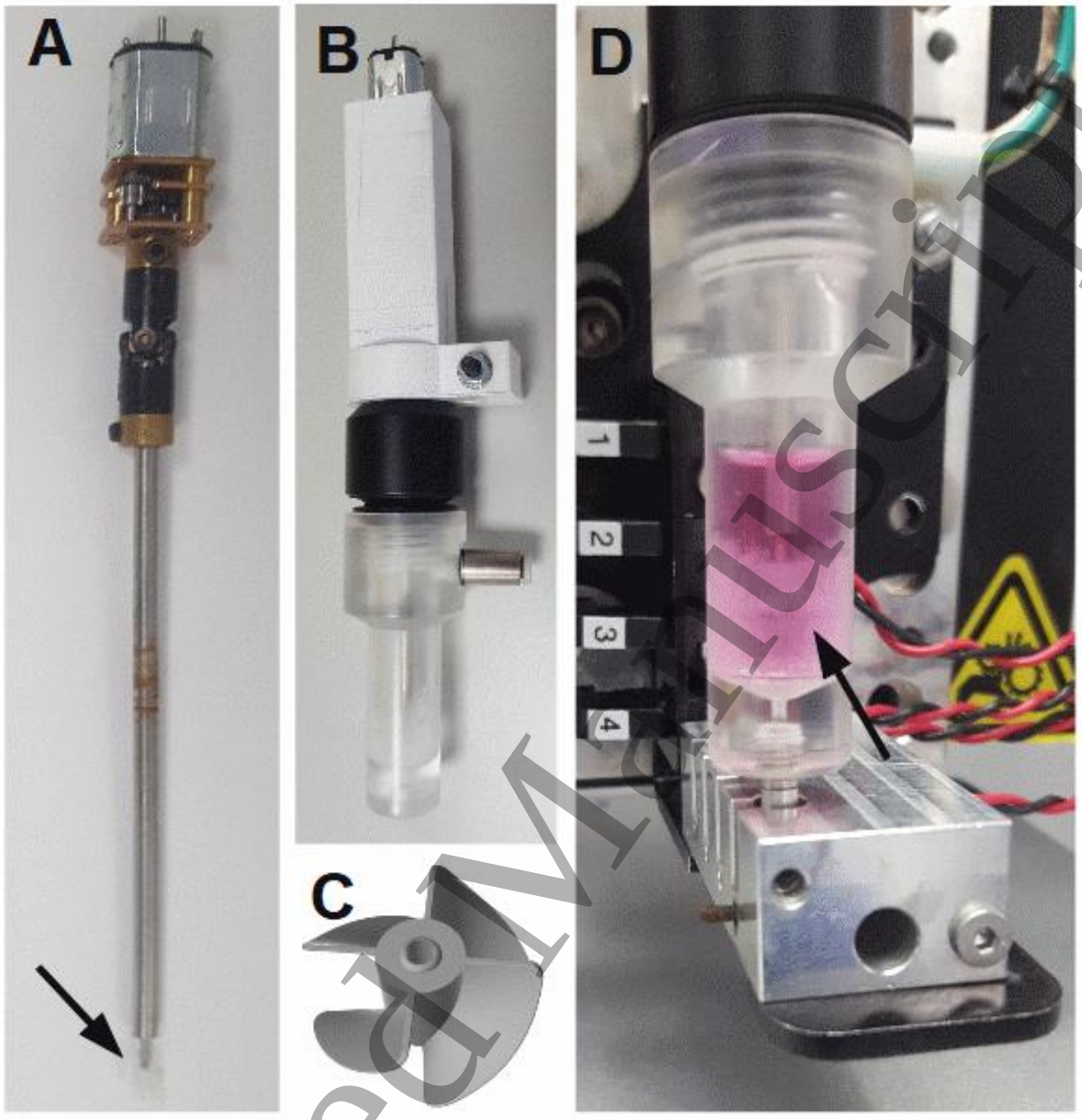

Figure 2 – Reservoir and agitator design 'A' used to minimise cellular aggregation during printing. (A) From top to bottom: motor, gearbox, driveshaft and impellor assembly (impellor indicated by a black arrow). (B) Reservoir and agitator following coupling. (C) Computer-aided design model of the impellor used to agitate the cell suspension. (D) Mounted device in a sealed configuration for printing. Under this configuration the inkjet actuator is encased in the mounting block immediately below the reservoir and agitation is achieved via rotation of the impellor. The overall length is 130 mm, and the impellor has a diameter of 8 mm and height of 4 mm.

Agitator Design B Diagram

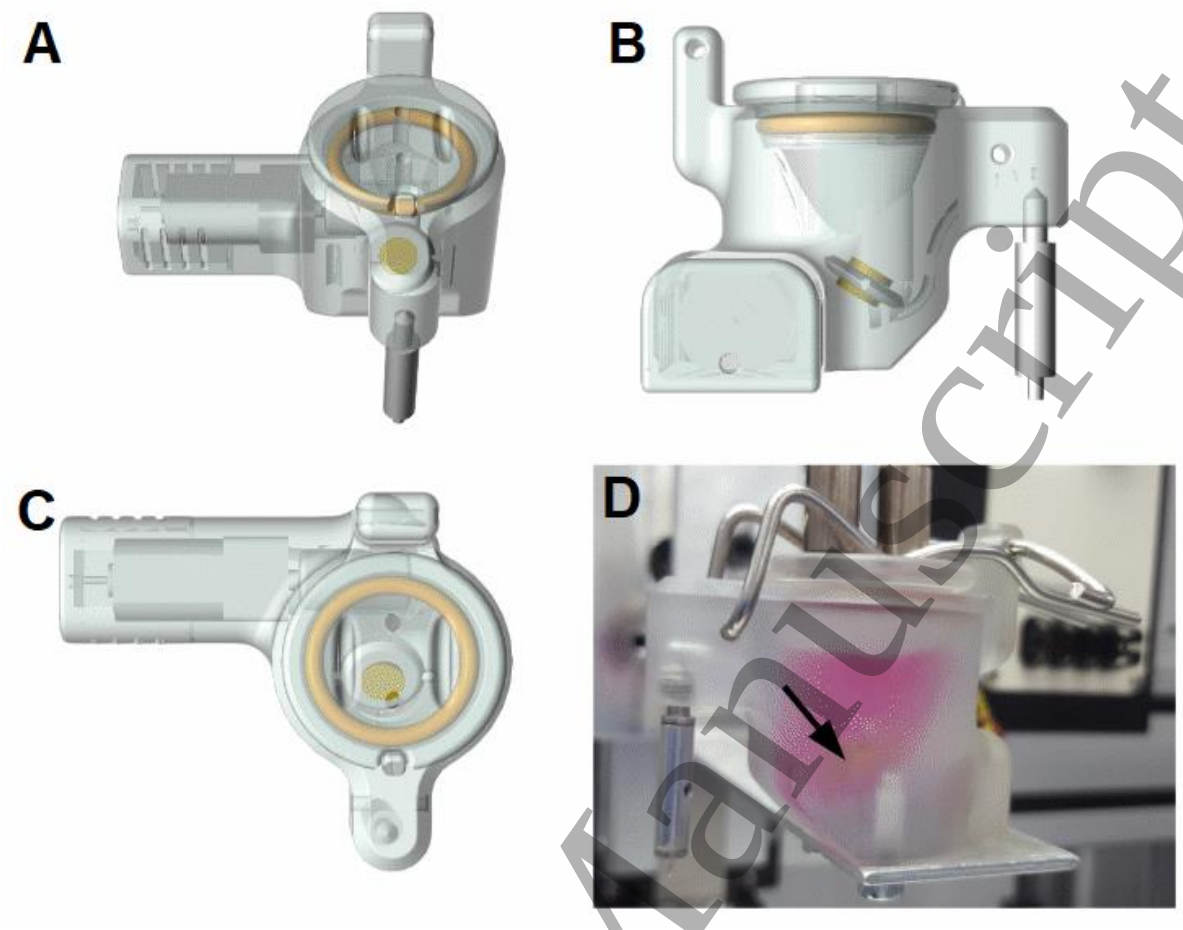

Figure 3 – Reservoir and agitator design 'B' used to minimise cellular aggregation during printing. (A) Front, (B) side and (C) top-down view of the computer-aided design model showing the reservoir assembly, motor, magnet (yellow) and chamber seal (orange) of the reservoir. (D) Mounted device in a sealed configuration for printing (magnet indicated by a black arrow). Under this configuration the inkjet actuator is suspended from the reservoir and agitation is achieved via rotation of the disk shaped magnet. The device has a length of 60 mm, height of 42 mm and depth of 48 mm. The magnet has a diameter of 8 mm and thickness of 3 mm.

Waveform Development

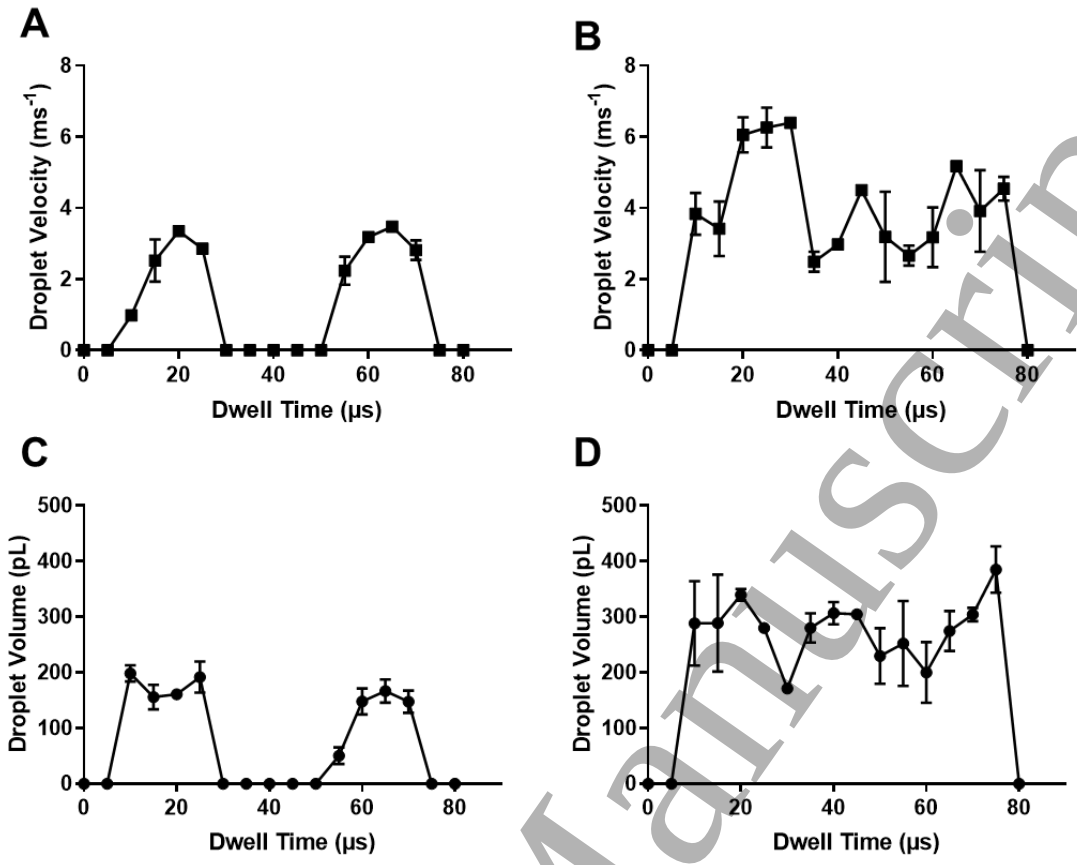

Figure 4 – Influence of dwell time on primary droplet ejection properties for unipolar and bipolar waveform designs at an actuation voltage of 40 V / -40 V. (A) Unipolar droplet ejection velocity. (B) Bipolar droplet ejection velocity. (C) Unipolar droplet ejection volume. (D) Bipolar droplet ejection volume. Data represents mean values ± SD. N=3.

Agitator Benchmarking

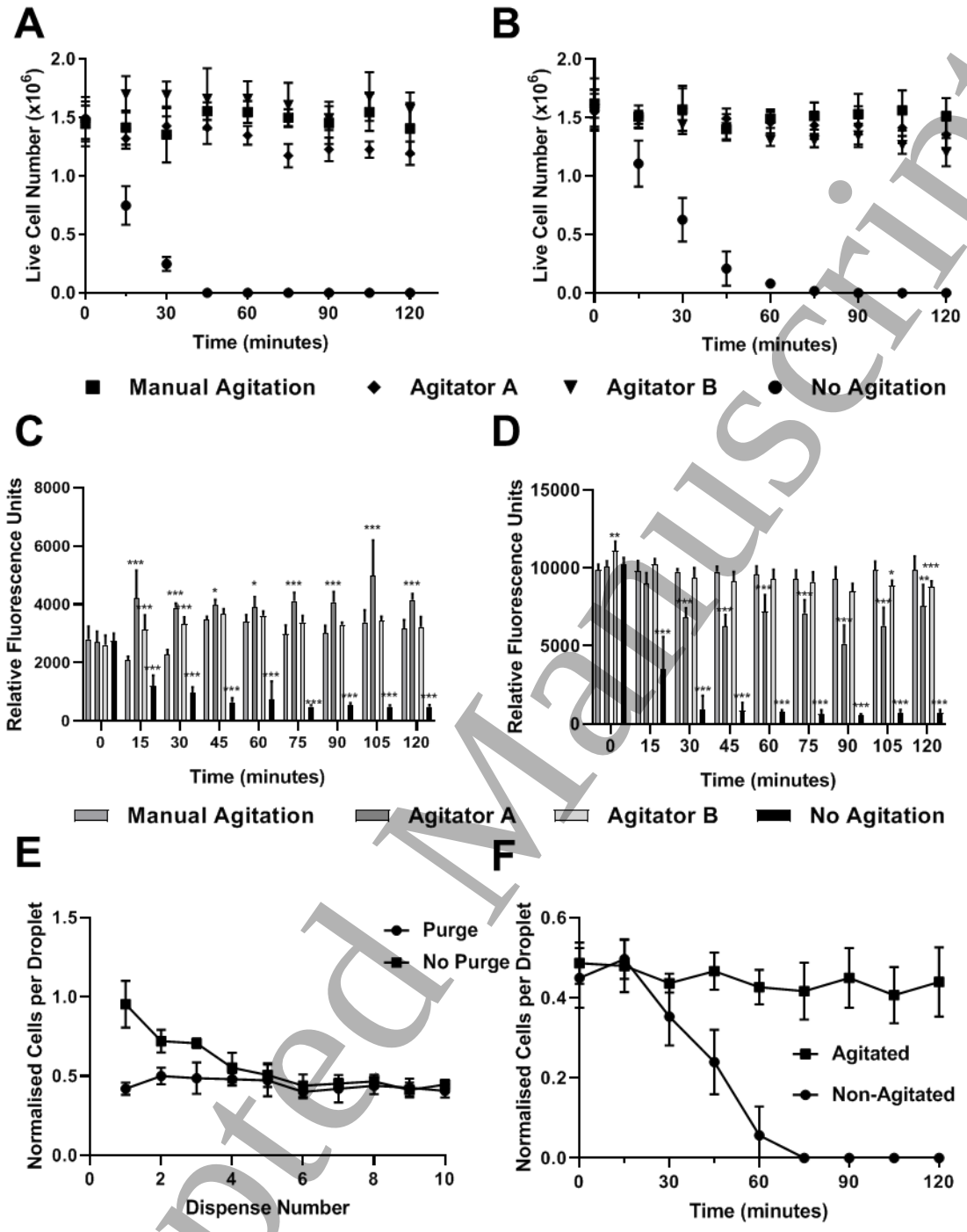

Figure 5 – Impact of reservoir agitation system on ink cellular dispersion and metabolic activity at a concentration of 10^6 cells per mL. (A) MSC count. (B) Chondrocyte cell count. (C) MSC metabolic activity. (D) Chondrocyte cell metabolic activity. (E) Effect of nozzle purging immediately prior to dispensing on cell density per sequentially ejected droplet. (F) Influence of agitation system on inkjet cell printing performance over a 2-hour printing period. Data represents mean values ± SD. N ≥ 3.

Nozzle Blockages

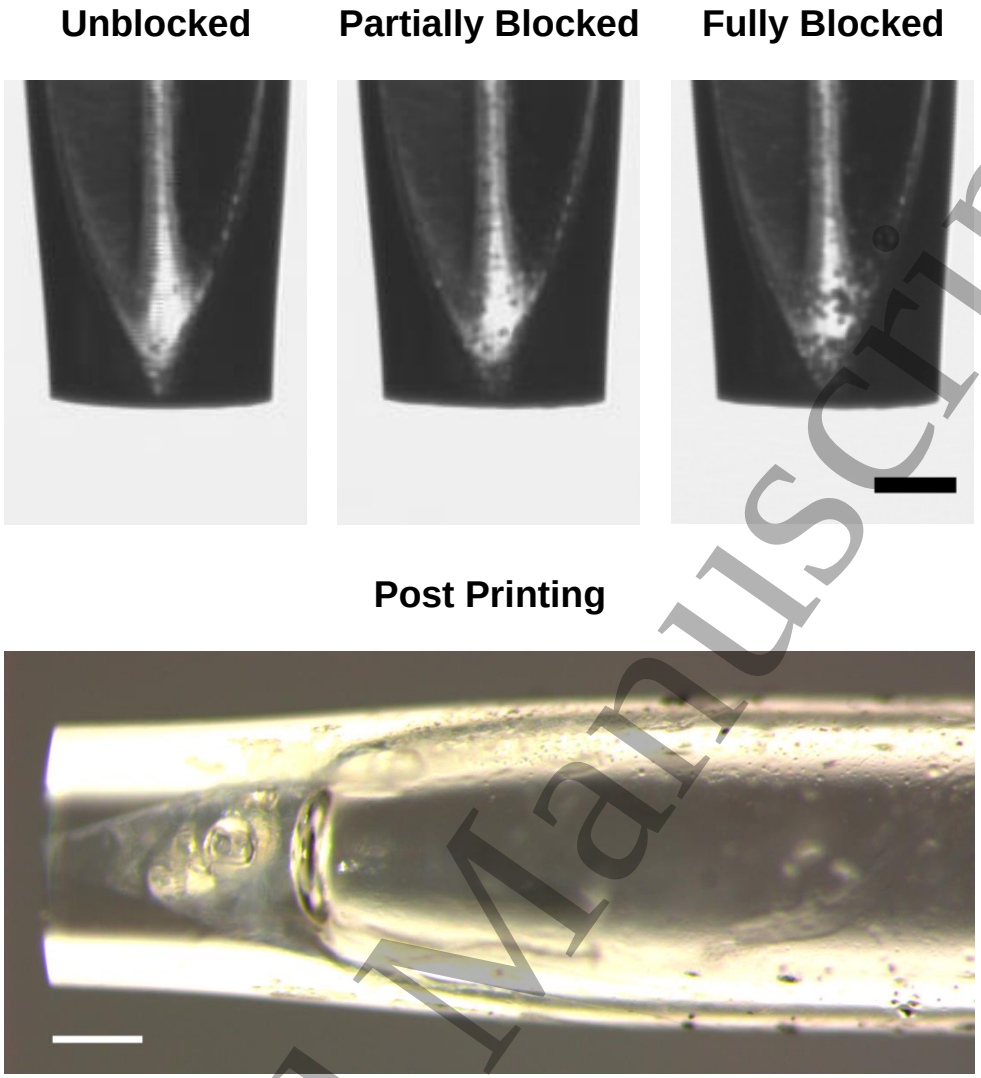

Figure 6 – Nozzle blockage and cell sedimentation captured using the JetLab® on-board stroboscopic camera (top) and via a microscope (bottom) when depositing ink at a concentration of 10^6 cells per mL in culture media. Scale bar = 200 µm.

Biological Impact Assessment

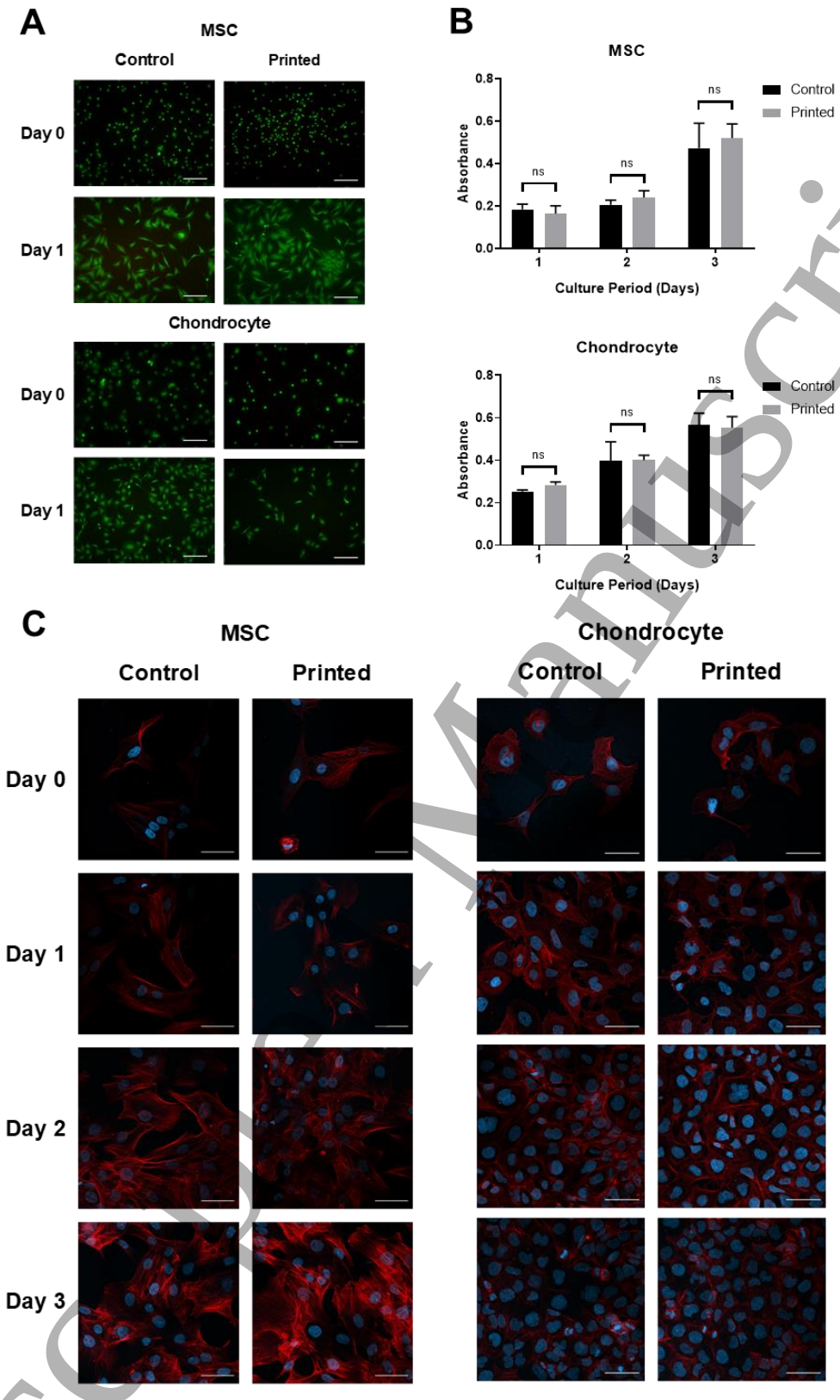

Figure 7 – Effect of printing process on the cellular viability and function of MSC and chondrocyte cell lines. (A) Cell viability assay showing live (green) and dead (red) cells. Scale bar = 200 µm. (B) Metabolic activity assay. Data represents mean values ± SD, N=6. (C) Cell morphology images showing cell nuclei visualised using DAPI (blue) and filamentous actin using phalloidin (red) staining. Scale bar = 50 µm.

Single Cell Printing Performance

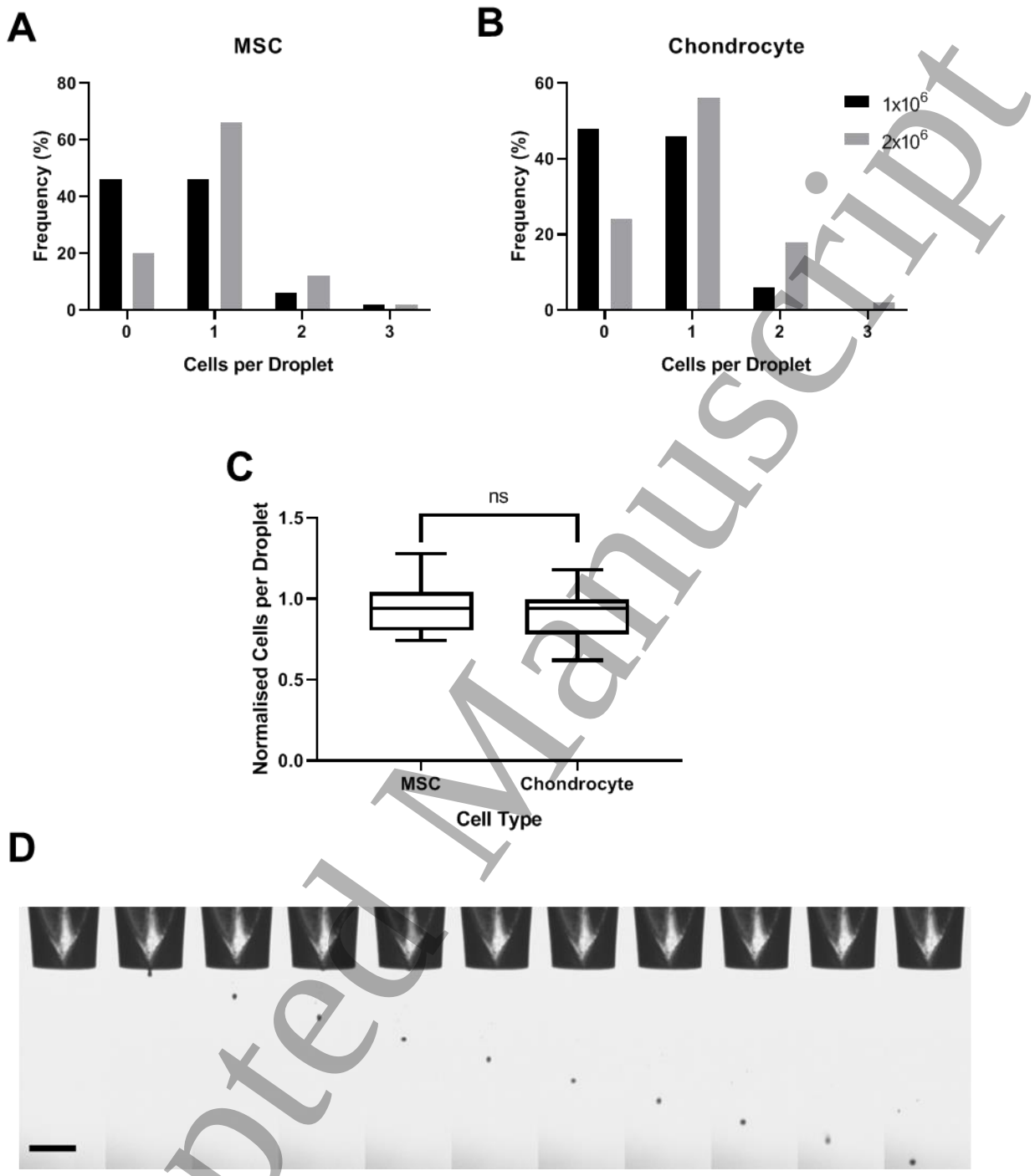

Figure 8 – Single cell printing performance when depositing MSC and chondrocyte cell lines. (A) Percentage of 50 sequentially deposited droplets containing different MSC concentrations at 1-2 x 10^6 cells per mL of cell culture media. (B) Percentage of 50 sequentially deposited droplets containing different chondrocyte cell concentrations at 1-2 x 10^6 cells per mL of cell culture media. (C) Mean cell density per droplet for each cell type. (D) Sequential droplet ejection images captured using the JetLab® on-board stroboscopic camera using an incremental strobe delay of 50 µs. Cells were deposited in cell culture media at a concentration of 1 million cells per mL. N=50. Scale bar = 400 µm.